Journal of Electroceramics, 13, 857–863, 2004
© 2004 Kluwer Academic Publishers. Manufactured in The Netherlands.

Effect of Nano-Scale Additions on the Enhancement of Superconductivity in Y-Ba-Cu-O Materials

SHIH-YUN CHEN,[1] IN-GANN CHEN,[1,*] PING-CHI HSIEH[1] & MAW-KUEN WU[2]

[1]*Department of Materials Science and Engineering, National Cheng Kung University, Tainan, Taiwan, Republic of China*
[2]*Institute of Physics, Academia Sinica, Taipei, Taiwan, Republic of China*

Submitted February 12, 2003; Revised March 6, 2004; Accepted April 30, 2004

Abstract. The coherence length of Y-Ba-Cu-O superconductor is in the nano-meter range, therefore, nano-scale additions can be used to increase the number of effective pinning centers in top-seed melt-growth (TSMG) Y-Ba-Cu-O single grain materials. Different kinds of nano-scale additions: Y_2O_3, and Y_2BaCuO_5 (Y211) were mixed with precursor powders ($YBa_2Cu_3O_7 + Y_2BaCuO$) followed by TSMG process in air. SEM and TEM were used to investigate the size and morphology of the 211-particles as well as the distribution of defects (e.g. dislocations) in the matrix. It was found that the size of 211-particles was slightly reduced in nm Y_2O_3 doped samples, and sub-micro 211-particles were observed in nmY211 doped samples. In addition, the critical temperature, T_c, for all samples was similar and independent of the type of addition, while the enhancement of critical current density, J_c(H, T), varied with the types of nano-scale addition. Accordingly, the reactions between the superconductive matrix and different nano-scale additions resulted in different pinning properties. These samples with different nano-scale additions were studied using scaling rule analysis to differentiate their pinning mechanisms. For comparison, the results of SmBCO samples with nano-scale additions are also discussed in this study.

Keywords: superconductivity, nano-scale, additions, pinning mechanism

1. Introduction

Melt-processed Y-Ba-Cu-O (YBCO) superconductor bulks have extensive potential for engineering applications. However, the J_c of YBCO decreases quickly with increasing the magnetic field, and the J_c of REBCO (RE: Sm or Nd) is better than YBCO bulks in high field regions. In order to enhance the YBCO's J_c-H performance, the number of effective pinning centers at high field should be increased. It has been reported that twins, point defects [1], dislocations [2], stacking faults [3] and the interface between non-superconducting phase (ex. 211-particles) and superconducting phase (123 matrix) can act as effective pinning centers [4]. Refinement of 211-particles can also induce the formation of defects in the nearby 123 matrix [5–7]. Therefore, J_c of superconductors can be improved by increasing the amount of small sized (sub-μm) 211-particles in the superconductors. Adding small amounts of additions [8–11] or using submicron 211-particle as precursor powders are both effective in reducing the 211-particles size.

However, the effect on enhancing pinning by the above mentioned pinning centers (the 123/211 interface and defects) is larger at low magnetic fields than at high magnetic fields [12]. In order to enhance the J_c at high magnetic fields, field-induced pinning centers are required. Recently, some researchers have reported that the artificially induced pinning centers using a nanoparticle route proved effective in enhancing J_c values. In BSCCO and MgB_2 materials, it has been reported that J_c and the irreversibility field were both increased by the addition of nano-ZrO_2 [13], nano-MgO [14], and nano-Y_2O_3 [15]. In SmBCO samples, J_c enhancement at a high field region was also reported by adding small amounts of nano-Sm211 and nano-Y_2O_3 [16]. The above nano additives improve the pinning ability by forming nano-sized composites (ex. Y_2O_3 react with MgB_2 to form YB_4 or react with Sm123 matrix

*To whom all correspondence should be addressed. E-mail: ingann@ mail.ncku.edu.tw

to form compositional fluctuations) or by acting as a column defect (ex. nano MgO rod).

In this study, two types of nano-scale particles were used: Y211 and Y_2O_3, in order to increase the number of small sized non-superconducting particles which were expected to act as effective pinning centers in the Y-Ba-Cu-O superconductors. The effect of these additions on pinning mechanisms was examined using scaling rule analysis of J_c-H measurements and by microstructural analysis. Meanwhile, SmBCO samples with small amounts of nano-Sm211 and Y_2O_3 were also investigated to compare the effect of nano-scale additives on YBCO samples and SmBCO samples.

2. Experimental Procedure

The Y123 and Y211 powders were prepared by the conventional solid-state calcination reaction of Y_2O_3, $BaCO_3$, and CuO powders, and the nano-scale 211-particles (nm211 particles) were prepared by the sol-gel method, while nano-scale Y_2O_3 was obtained commercially. The size distribution of nano-scale particles was measured by the particle size distribution analyzer (*zetasizer*/1000), and showed the mean diameters for the nm211 and Y_2O_3 to be 50 nm and 27 nm, respectively. The mixture of precursor powders (Y123 + 15 wt% Y211) with the addition of 0.1 to 1 wt% nano-scale particles (as listed in Table 1) was pressed and processed in an isothermal box furnace. The YBCO (Y-Ba-Cu-O) samples were grown by a typical top-seeded melt-textured (TSMT) method. The TSMT grown specimens were annealed in flowing oxygen at 300°C for 200 hrs. The DC magnetization measurements were carried out using a superconducting quantum interference device magnetometer (SQUID, Quantum Design MPMS7) to determine the T_c and J_c (H, T). The T_c results were measured by zero-field-cooling (ZFC) followed by exposure to a 10 Oe magnetic field. The J_c (amp/cm^2) values were estimated according to the extended Bean model using the following equation:

$$J_c = 20(\Delta M)/a(1 - a/3b) \quad (1)$$

where ΔM (emu/cm^3) is the magnetization hysteresis, a and b (cm) are the cross-sectional dimensions of the sample perpendicular to the applied field and $a < b$. The microstructural observations were performed with SEM (PHILIPS XL-40 FEG SEM) and TEM (HITACHI HF-2000).

Table 1. The amount of additions and the T_c of the samples with different nano scale additives.

Sample	nm-Y211 (wt%)	Y_2O_3 (wt%)	T_{conset}[a] (K)	T_c[b] (K)	ΔT_c[c] (K)
YBCO					
Control (un-doped)	0	0	91	89	1
0.01	0.01	0	92	89	1
0.1	0.1	0	92	89	2
1	1	0	91	89	1
0.01	0	0.01	92	90	2
0.1	0	0.1	91	89	1
1	0	1	92	90	1
SmBCO					
Control (un-doped)	0	0	89	87	5
0.1	0.1	0	93	89	2
1	1	0	94	92	1
0.1	0	0.1	94	91	2
1	0	1	94	92	1

[a]The temperature where M becomes negative (i. e. diamagnetism).
[b]The temperature of the dM/dT peak, i.e. the highest diamagnetism transition rate.
[c]The full width at half max in the dM/dT vs. T curve.

3. Results and Discussion

3.1. Superconductivity

Table 1 shows the T_c results for the YBCO samples with different amounts of nano-scale addition. The T_c values for all the nmY_2O_3 and nmY211 doped samples are in the same range of $T_c \sim 90$ K, which indicates that the addition did not destroy the superconductive Y123 matrix structure.

3.2. J_c-H Measurement

3.2.1. Y-Ba-Cu-O System. Figure 1 shows the J_c-H curves of the un-doped (named control below) and nmY_2O_3 doped samples at (a) 65 K and (b) 77 K with the applied magnetic field parallel to the c axis. It is seen that the highest J_c values are in the 0.01 wt% sample, and the J_c-H curves decrease with increasing the amounts of nmY_2O_3 addition. At a low magnetic field, the J_c-H curves of 0.01 wt% nmY_2O_3 doped samples are larger than that of the control sample, while in the higher doped samples (0.1 wt%, 1 wt%), the J_c-H curves are similar to the control sample. With increasing the magnetic field, a peak was observed in the nmY_2O_3 doped samples at 65 K, and the peak position shifted to low field regions with increasing the amount

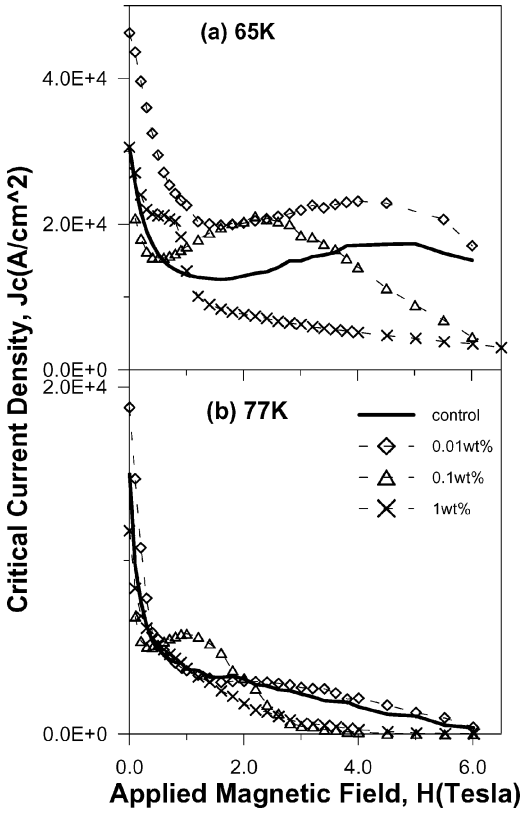

Fig. 1. J_c (H, T) H//c measurements of different amounts of nmY_2O_3 doped YBCO samples at different temperatures.

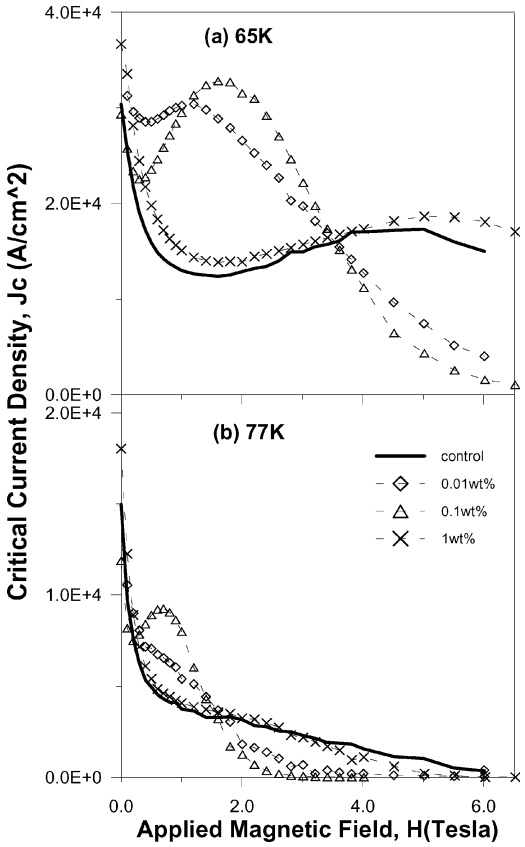

Fig. 2. J_c (H, T) H//c measurements of different amounts of nmY211 doped YBCO samples at different temperatures.

of addition. At 65 K, the peak position was $4T$, $2T$, and $1T$ for the 0.01, 0.1 and 1 wt% sample respectively. At 77 K, the peak effect disappeared for all samples, except for the 0.1 wt% sample which had a peak position of $\sim 1T$. Therefore, it can be conjectured that the influence of the nmY_2O_3 addition is both the increase of pinning centers act in low fields and the formation of peak effect. However, the enhancement in J_c is not significant with nmY_2O_3 addition, especially at high temperatures (77 K).

As for the effect of nmY211 additions, as shown in Fig. 2, the relation between J_c and magnetic field of nmY211 doped samples is quiet different to that of the control samples. As mentioned before, J_c for the control sample decreased with increasing the magnetic field. In the nmY211 doped sample, the J_c values in low field regions were similar to the control sample, but a significant peak was observed in the field range from 1 to $3T$ at 65 K, especially for the 0.1 wt% nmY211 doped sample. This is the first time that such a large peak has been observed in YBCO samples. At a higher temperature (77 K) or with higher amounts of nmY211 addition, the peak effect weakens, but the J_c-H curves of the 0.1 wt% nmY211 doped samples are still enhanced in the intermediate field range (from 0.2 to $1.5T$). Additionally, it is worthy to note that the J_c-H performance for the 0.01 and 0.1 wt% nmY211 doped samples deteriorated drastically in the high field regions, while for the 1 wt% doped sample, it was similar to that of the control sample.

Regarding the origin of the peak effect, it has been reported that in REBCO materials, the nano-sized RE-rich clusters (or compositional fluctuations) act as field pinning centers, and thus enhance the J_c performance in the high field region. In contrast, in the YBCO system, the peak effect is not as obvious as that of the REBCO system. However, some researchers also indicated that oxygen deficiency and the localized mis-match strain may result in the intermediate peak. In this study, the

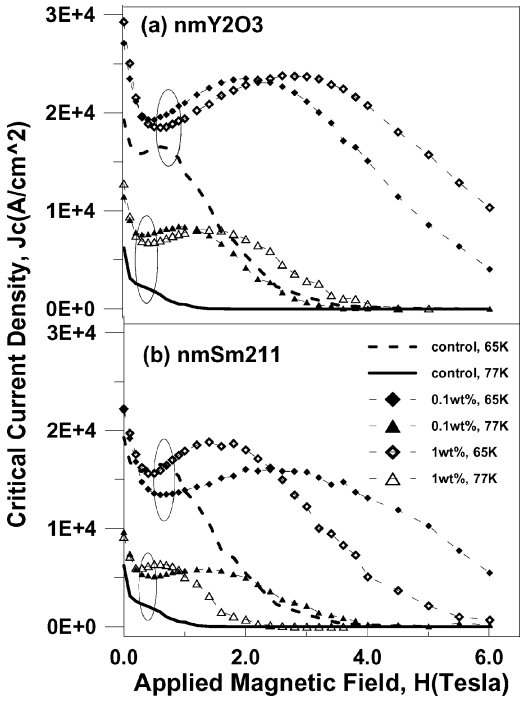

Fig. 3. J_c (H, T) H//c measurements of SmBCO samples with different types of additions at different temperatures, (a) control, (b) nmY_2O_3 and (c) nmSm211.

peak observed in YBCO samples is contributed by the nmY_2O_3 and nmY211 additions. The reactions of these two types of additives have been investigated in SmBCO system.

3.2.2. Sm-Ba-Cu-O system. As shown in Fig. 3(a), in the nmY_2O_3 doped SmBCO samples, the J_c-H curves were enhanced over a wide field region. At 65 K, the J_c enhancing reached $6T$; at 77 K, the J_c enhancing reached $4T$. A significant peak was observed at a high magnetic field and the peak width and peak position were a little larger with higher amounts of nano-scale precursor addition. Combined with the microstructural observations, it has been proposed [16] that there are two types of reaction between the Sm123 matrix and nmY_2O_3 addition: (i) nmY_2O_3 addition remains as particles in the matrix and (ii) nmY_2O_3 addition reacts with matrix and forms regions with compositional fluctuations which may be expressed as (Sm, Y)$Ba_2Cu_3O_7$. The former type results in an enhanced J_c in low field regions, and the latter one results in enhancement in high field regions.

As for the SmBCO samples with nmSm211 addition (as shown in Fig. 3(b)), the J_c-H curves in the low field are similar to that of the control sample, but in the high field, the J_c-H curves show a peak effect. Based on the growth mechanism of MTG process, it is known that the 123 phase grows according to the following peritectic transformation:

$$RE_2BaCuO_{5(s)} + \text{Liq.}(3\ BaCuO_2 + 2\ CuO) \rightarrow 2\ RE_{1+x}Ba_{2-x}Cu_3\mathbf{O}_{6(s)} \quad (2)$$

211-particles with larger curvatures exhibit higher compositional difference (ΔC) between Liquid/211, thus small sized 211-particles in liquid with large curvature will dissolve faster than the larger ones. The 211-particle size distribution showed the number of small sized 211-particles ($<1\ \mu$m) found in the matrix after MTG process ranges in the same order of magnitude for the control and the nm211 doped samples. Therefore, it can be conjectured that most nm211 additions would have dissolved during the MTG process, and become nano-sized regions with compositional fluctuations (Δx) in the $RE_{1+x}Ba_{2-x}Cu_3O_6$ matrix that provide the sources of $\Delta\kappa$ pinning [17].

In the present system (YBCO), samples with small amounts of nmY_2O_3 addition (0.01 wt%, 0.1 wt%) with peaks in a high magnetic field ($>2\ T$ at 65 K) were observed, thus, the reactions between Y123 matrix and nmY_2O_3 addition may be similar to that of SmBCO samples. But in the nmY211 doped YBCO samples, the change on J_c is mainly in intermediate fields ($<2T$ at 65 K), therefore, the pinning of nmY211 doped YBCO samples may be different to the nmSm211 doped SmBCO samples.

3.3. Pinning Mechanism

In order to differentiate the pinning mechanisms of the control samples, nmY_2O_3 doped and nmY211 doped samples, scaling rule analysis was used. The general expression of the volume pinning force $F_p(H)$ which was proposed by Dew-Hughes [18] is expressed in the form:

$$F_p/F_{p,\max} \propto h^p(1-h)^q \quad (3)$$

where $F_{p,\max}$ is the maximum volume pinning force, h is the reduced field (H/H_{irr}), and the parameters p

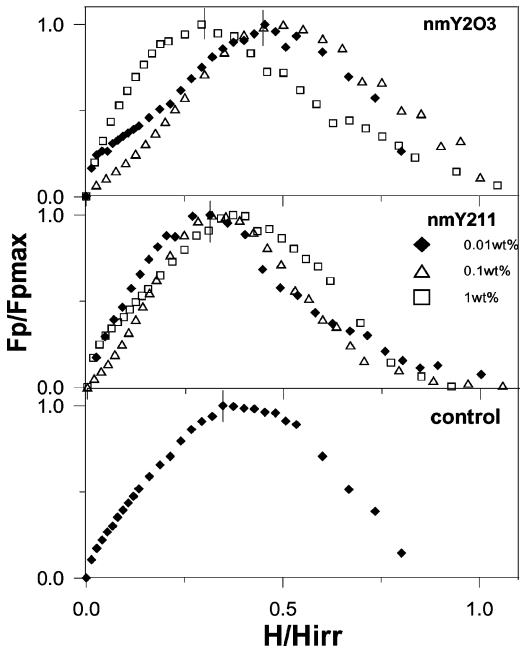

Fig. 4. Normalized pinning force $F_p/F_{p,\max}$ versus $H/H_{\rm irr}$ at 77 K for (a) control sample, (b) nm Y_2O_3 doped, (c) nm Y211 doped samples. The segments indicate the $h_{\max}$.

and q depend on the characteristics of flux pinning. Two different sources of pinning have been reported: one is a non-superconducting defect embedded in the superconducting matrix (normal pinning), the other is a spatial variation of the Ginzburg-Landau parameter in the superconductivity matrix ($\Delta\kappa$ pinning). Notably, a large $h_{\max}$ value ($\sim$0.5) represents $\Delta\kappa$ pinning and a small $h_{\max}$ value $\sim$0.33 represents normal pinning [19].

The pinning force F_p versus the reduced field h ($H/H_{\rm irr}$) for the control and nano-scale additive samples at 77 K is plotted in Fig. 4. Among these samples, the $F_p - h$ curves are basically similar in both the values of $h_{\max}$ and the relationship between magnetic fields for all samples, except for the 0.01 and 0.1 wt% nmY_2O_3 doped samples. In most of the samples, including the control, nmY211 doped, and 1 wt% nm Y_2O_3 doped samples, the $h_{\max} \sim 0.33$ and the curves follow normal point pinning; while in the 0.01 and 0.1 wt% nmY_2O_3 doped samples, $h_{\max} \sim 0.40$–0.45 and the curves follow a combination of normal pinning and $\Delta\kappa$ pinning. Accordingly, the enhanced pinning in the nmY211 doped samples is related to the formation of non-superconductive defects in the Y123 matrix. As for the nmY_2O_3 doped samples, certain reactions between the nmY_2O_3 and Y123 matrix would induce T_c(H) variation that resulted in $\Delta\kappa$ pinning. Notably, with further increasing the amount of nmY_2O_3 addition, the effect of $\Delta\kappa$ pinning disappeared.

3.4. Microstructure Observation

SEM observations found that the 211-particle size for nmY_2O_3 doped samples was smaller than the control and nmY211 doped samples. TEM micrographs found that in the nmY_2O_3 doped samples, some small particles existed inside the 211-particles (as shown in Fig. 5(a)). EDS results showed that the stoichiometry

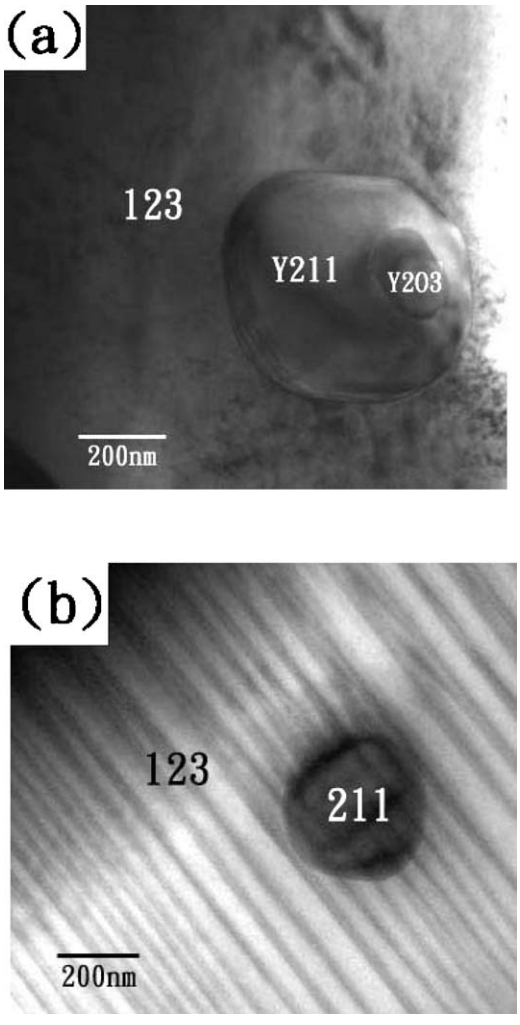

Fig. 5. TEM micrographs of YBCO samples with different nano-scale additions. (a) nmY_2O_3 doped samples: small Y_2O_3 particles exist inside the 211-particles. (b) nmY211 doped samples: small sized (sub-micro) 211-particles were found in the matrix.

of the embedded small particles was similar to that of Y_2O_3. This agrees with the theory that Y_2O_3 particles can act as nuclei sites for 211-particles and thus the 211-particle size can be reduced. As a consequence, the interface pinning is stronger and thus the J_c-H curves of the nmY_2O_3 doped sample were enhanced, especially in low field regions ($<0.5T$ at 77 K). However, the enhancement in J_c is not significant with nmY_2O_3 addition, especially at high temperatures (77 K). In addition, it is also found that the J_c-H performance from high to low is in the sequence of 0.01, 0.1, and 1 wt%. This can be attributed to the distribution of nmY_2O_3 in the matrix. However, it is noted that although the values are higher, the J_c-H performance for the 0.01 wt% nmY_2O_3 doped sample is similar to that of control sample. With increasing the amount of nmY_2O_3 addition, the peak in the intermediate field region became more significant. The pinning analysis ($F_p - H$) also found the change of pinning mechanism in the higher doped samples (the h_{max} in the 0.1 and 1 wt% nmY_2O_3 doped samples is $\sim$0.4, which is higher than that of the control and 0.01 wt% nmY_2O_3 doped samples.). Therefore, it can be conjectured that the influence of the nmY_2O_3 addition is both the increase of pinning centers act in low fields and the formation of peak effect which may have resulted from the inter-diffusion between the nmY_2O_3 additives and matrix during the MTG process. Further study is still under progress.

As for the nmY211 doped samples, the SEM microstructures were similar to the control sample. TEM results found that in the Y123 matrix, the number of small sized 211-particles (as shown in Fig. 5(b)) was larger than that of the control sample, but still smaller than that in the precursor (the mean diameter was 50 nm for the nmY211 additions, the composition of the precursors is Y123 + 15 wt%Y211 + 0.01 wt%, 0.1 wt%, 1 wt% nmY211, as listed in Table 1). Therefore, it can be deduced that the nmY211 addition dissolve during the peritectic reaction as mentioned in 3.2.2. However, the J_c results and $F_p - H$ analysis of the nmY211 doped samples show that the enhancing of J_c by nmY211 addition was mainly in intermediate fields and the dominant pinning was normal pinning, which are different to those of SmBCO samples. It is known that the solid solubility of Y atom in the Y123 is much less than that of Sm in the Sm123. Therefore, it can be deduced that the origin of the peak for the nmY211 doped samples was the dissolving of nmY211 additions, which probably resulted in regions with higher Y content which induced oxygen deficiencies and defects in the matrix. On the other hand, the different dissolubility of Y and Sm atoms which has been reported by Shiohara et al. [22] also related to the different results of nm211 additions on J_c between SmBCO and YBCO samples. Shiohara et al. indicated that at high temperatures ($\sim$1400 K), the dissolubility of Sm is about 3 times that of Y. Accordingly, the degree of compositional fluctuations caused by the dissolution of nm211 additions at high temperatures was larger for the SmBCO samples than the YBCO samples, which resulted in the larger difference of T_c for the SmBCO samples. So, in the SmBCO samples, the nmSm211 addition is related to the formation of $\Delta\kappa$ pinning centers while in the YBCO samples, the contribution to J_c from $\Delta\kappa$ pinning is significantly less than that of normal pinning. In addition, it can be conjectured that the reactions between nmY211 and matrix also resulted in the degradation of J_c in high field regions in the 0.01 and 0.1 wt% doped samples. The dissolution of nmY211 changes the stoichmetry and oxygen deficiency of the matrix, which may influence the pinning behavior at different magnetic field.

Our current results indicate that J_c-H curves are changed with small amounts of nano-scale Y_2O_3 (0.01 wt%) and Y211 (0.01, 0.1 wt%) additions, especially in the intermediate field for the nmY211 doped samples. However, the enhancement is much more significant at lower temperatures. These additives react with the matrix during the MTG process. We believe that combined addition with optimized amount of other additives will result in even higher J_c values.

4. Conclusions

The superconductivity and microstructure of MTG YBCO samples with the addition of small amounts of nano-scale additives: Y_2BaCuO_5 (nmY211) and Y_2O_3 was investigated. These two kinds of additions reacted with Y123 matrix during MTG process. The Y_2O_3 particles acted as nuclei sites for 211-particles and nmY211 dissolved. The J_c values were enhanced for samples with nmY_2O_3 addition, and a significant peak was observed in the intermediate field for the small amounts of nmY211 doped samples. As for the different results of nm211 additions on J_c between YBCO and SmBCO, this may be related to the different dissolubility of Y and Sm atoms from the solid to the liquid phase and the different solid solubility of RE atom in RE123 phase.

Acknowledgment

This research is supported by the National Science Council, Republic of China, Taiwan, under the contact No. NSC-91-2112-M-006-031.

References

1. N. Chikumoto, M. Konczykowski, K. Kishio, and M. Murakami, *Physica C*, **282–287**, 2143 (1997).
2. J. Mannhart, D. Anselmetti, J.G. Bednorz, Ch. Gerber, K.A. Muller, and D.G. Schlom, in *Proc. 6th Int. Workshop on Critical Currents in High-TC Supercond*., Cambridge, UK (1991) p. 5242.
3. R. Ramesh, S. Jin, S. Nakahara, and T.H. Tiefel, *Appl. Phys. Lett*., **57**, 1458 (1990).
4. D.F. Lee, V. Selvamanickam, and K. Salama, *Physica C*, **202**, 83 (1992).
5. Z.L. Wang, A. Goyal, and D.M. Kroeger, *Physical Review B*, **47**, 5373 (1993).
6. M. Mironova, D.F. Lee, and K. Salama, *Physica C*, **211**, 188 (1993).
7. S.Y. Chen, P.C. Hsieh, and I.G. Chen, Accepted for Publication in IEEE Trans. On Applied. Superconductivity.
8. M. Hussain, S. Kuroda, and K. Takita, *Physica C*, **297**, 176 (1998).
9. G. Karabbes, G. Fuchs, P. Schatzle, S. Grub. J.W. Park, F. Hardinghaus, G. Stover, R. Hayn, S.-L. Drechsler, and T. Fahr, *Physica C*, **330**, 181 (2000).
10. S. Pinol, F. Sandiumenge, B. Martinze, V. Gomis, J. Fontcuberta, and X. Obradors, *Appl. Phys. Lett*., **65**(11), 1994.
11. C.-J. Kim, K.-B. Kim, D.-Y. Won, H.-C. Moon, D.-S. Suhr, S.H. Lai, and P.J. McGinn, *J. Mater. Res*. **9**, 1952 (1994).
12. M. Murakami, *Melt Processed High-Temperature Superconductors* (World Scientific Publishing Co. Pte. Ltd, 1992).
13. Z.Y. Jia, H. Tang, Z.Q. Yang, Y.T. Xing, Y.Z. Wang, and G.W. Qiao, *Physica C*, **337**, 130 (2000).
14. P. Yang and C.M. Lieber, *Science*, **273**, 1836 (1996).
15. J. Wang, Y. Bugoslavsky, A. Berenov, L. Cowey, A. Caplin, L.F. Cohen, L.D. Cooley, X. Song, and D.C. Larbalestier, *Appl. Phys. Lett*., **81**(11), 2026 (2002).
16. S.Y. Chen, P.C. Hseih, and I.G. Chen, submitted to *Superconductor Science and Technology*.
17. S.Y. Chen, P.C. Hseih, I.G. Chen, and M.K. Wu, accepted for publication in *J. Mater. Res*.
18. D. Dew-Hughes, *Philos. Mag*., **30**, 293 (1974).
19. M.R. Koblischka, A.J.J. van Dalen, T. Higuchi, S.I. Yoo, and M. Murakami, *Physica Review B*, **58**(5), 2863 (1998).
20. O.B. Hyun, M. Yoshida, T. Kitamura, and I. Hirabayashi, *Physica C*, **258**, 365 (1996).
21. E. Sudhakar Reddy, K.D. Otzschi, J. Shimoyama, and K. Kishio, *Physica C*, **361**, 114 (2001).
22. X. Yao and Y. Shiohara, *Superconductor Science and Technology*, **10**, 249 (1997).